12th International Conference on Information Fusion
Seattle, WA, USA, July 6-9, 2009

Target Tracking in Heavy-Tailed Clutter Using Amplitude Information

Edmund F. Brekke
University Graduate Center
Kjeller, Norway.
edmund@unik.no

Oddvar Hallingstad
University Graduate Center
Kjeller, Norway.
oh@unik.no

John H. Glattetre
Kongsberg Maritime
Horten, Norway.
jhg@kongsberg.com

Abstract – *Harbor surveillance above and below the sea surface depends on sensors such as surveillance radar and multibeam sonar. These sensors attempt to detect and track moderately observable targets such as small boats or human divers in environments which often are characterized by heavy-tailed backgrounds. Target tracking in heavy-tailed environments is challenging even for moderately strong targets due to the more frequent occurrences of target-like outliers. One strategy for increased robustness is to use the backscattered signal strengths together with the kinematic measurements in the tracking method. This paper proposes two new amplitude likelihoods for target tracking in heavy-tailed backgrounds. The first likelihood works by incorporating the uncertainty of the background estimate. The second likelihood explicitly treats the background as heavy-tailed using the K-distribution.*

Keywords: Data association, Detection, Feature Aided Tracking

1 Introduction

In harbor surveillance sensors such as radars and sonars are used to detect and track various targets. The sensor provides an array of observations to be further analyzed through signal processing and data analysis. After preprocessing, such as matched filtering, a detector is employed to extract point measurements from the array. This is done by setting a threshold according to a Constant False Alarm Rate (CFAR) criterium [9]. Then tracks are established and maintained by feeding these extracted point measurements to a target tracking method.

The targets we have in mind are small boats in radar data or human divers in sonar data. Both can be expected to have a Signal to Noise Ratio (SNR) somewhere between $0\mathrm{dB}$ and $20\mathrm{dB}$. This means that if the target is to be detected with a reasonably high probability one must allow some false alarms to occur. In order to establish and maintain a track on such a target one must determine which detections are actually from the target, and which detections are to be considered as false alarms or clutter.

A popular solution to this problem of data association is found in the Probabilistic Data Association Filter (PDAF) and its multi-target version Joint Probabilistic Data Association Filter (JPDAF) [4]. One way to improve the performance of the PDAF is the utilization of Amplitude Information (AI). In [11] the PDAFAI (PDAF with Amplitude Information) was therefore presented. While the PDAF only uses kinematic measurements $z_k(i)$, the PDAFAI also uses the corresponding amplitudes $a_k(i)$ in order to decide which measurement is most likely to originate from the target. Of course the utilization of AI can be incorporated in other tracking methods as well. Although AI-based tracking methods have been around for some time, the usage of AI does not appear to be commonplace in practical systems.

Figure 1 illustrates the difference between the conventional PDAF and the PDAFAI. It is meant to highlight the fact that the two methods primarily differ in the data association part, and not in the state estimation part. Both methods calculate a conditional state estimate $\hat{\boldsymbol{x}}_{k|k}(i)$ for each measurement based on purely kinematic information. The PDAF solely depends on this kinematic information in the process of lumping these conditional state estimates together to the final a posteriori state estimate $\hat{\boldsymbol{x}}_{k|k}$. The PDAFAI uses the amplitudes of the measurements as well in this process. Since the PDAFAI has access to more information than the PDAF, it can be expected to outperform the PDAF, as long as the background and target amplitude statistics are adequately modeled.

Most work on AI assumes that the background is Gaussian or Rayleigh distributed [11,14] with a known power. Such assumptions may or may not be adequate in the real world. Experimental evidence [1] has indicated that more heavy-tailed background models should be considered. In particular, the K-distribution [15] is popular in the radar and sonar communities.

Many papers have been published on detectors in heavy-tailed clutter, see for example [3] or [8]. However, such papers make no mention of *target tracking*. This is problematic, as a detection system in heavy-tailed noise may need to operate at high false alarm rates ($\approx 10^{-2}$). The decision as

Report Documentation Page

Form Approved
OMB No. 0704-0188

1. REPORT DATE	2. REPORT TYPE	3. DATES COVERED
JUL 2009		**06-07-2009 to 09-07-2009**

4. TITLE AND SUBTITLE	5a. CONTRACT NUMBER
Target Tracking in Heavy-Tailed Clutter Using Amplitude Information	5b. GRANT NUMBER
	5c. PROGRAM ELEMENT NUMBER
6. AUTHOR(S)	5d. PROJECT NUMBER
	5e. TASK NUMBER
	5f. WORK UNIT NUMBER
7. PERFORMING ORGANIZATION NAME(S) AND ADDRESS(ES) **University Graduate center,Kjeller, Norway, , ,**	8. PERFORMING ORGANIZATION REPORT NUMBER
9. SPONSORING/MONITORING AGENCY NAME(S) AND ADDRESS(ES)	10. SPONSOR/MONITOR'S ACRONYM(S)
	11. SPONSOR/MONITOR'S REPORT NUMBER(S)

12. DISTRIBUTION/AVAILABILITY STATEMENT
Approved for public release; distribution unlimited

13. SUPPLEMENTARY NOTES
See also ADM002299. Presented at the International Conference on Information Fusion (12th) (Fusion 2009). Held in Seattle, Washington, on 6-9 July 2009. U.S. Government or Federal Rights License.

14. ABSTRACT
Harbor surveillance above and below the sea surface depends on sensors such as surveillance radar and multibeam sonar. These sensors attempt to detect and track moderately observable targets such as small boats or human divers in environments which often are characterized by heavy-tailed backgrounds. Target tracking in heavy-tailed environments is challenging even for moderately strong targets due to the more frequent occurrences of target-like outliers. One strategy for increased robustness is to use the backscattered signal strengths together with the kinematic measurements in the tracking method. This paper proposes two new amplitude likelihoods for target tracking in heavytailed backgrounds. The first likelihood works by incorporating the uncertainty of the background estimate. The second likelihood explicitly treats the background as heavytailed using the K-distribution.

15. SUBJECT TERMS

16. SECURITY CLASSIFICATION OF:			17. LIMITATION OF ABSTRACT	18. NUMBER OF PAGES	19a. NAME OF RESPONSIBLE PERSON
a. REPORT	b. ABSTRACT	c. THIS PAGE			
unclassified	**unclassified**	**unclassified**	**Public Release**	**8**	

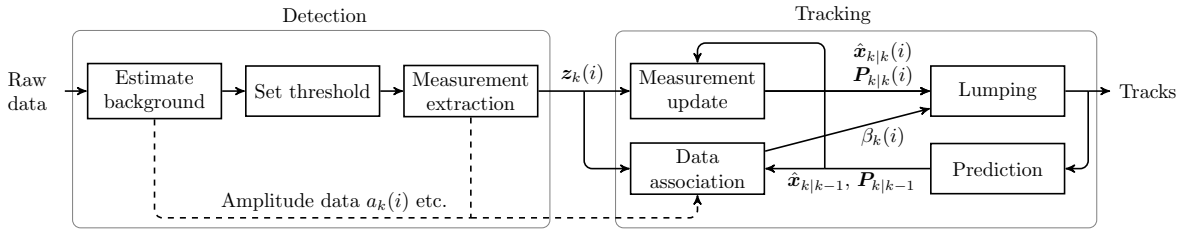

Figure 1: Schematic description of the PDAF and PDAFAI methods. The dashed connection represents the flow of amplitude information from detector to tracker, which only is present in the PDAFAI.

to whether the target is present or not can obviously not be made based on the detection process alone.

One way to overcome this challenge is to integrate the data before the detection decision is made, as done in so-called Track-Before-Detect (TBD) [5,14]. For very low SNR, when the target return cannot be expected to exceed any reasonable threshold, this is the only feasible approach to target tracking. Otherwise TBD is not worthwhile the very large computational expenses.

In [5] it was observed that effects similar to the well known phenomena of CFAR loss [9] could deteriorate the performance of TBD methods. Since TBD only relies on amplitude information, it is more sensitive to the interpretation of the background than conventional tracking methods. To prevent the method from being misled by misinterpretation of the background it was necessary to make its amplitude likelihood more conservative. This was done by marginalizing over the true, but unknown, noise parameter.

This paper presents further work on conservative amplitude likelihoods. While [5] focused on TBD methods, this paper focuses on more traditional PDAF and PDAFAI methods. Analogous to what was done in [5] we first develop a proper treatment of uncertain, but Rayleigh distributed, background noise. Then we establish the treatment of amplitude information in the more challenging case of heavy-tailed clutter.

The paper is organized as follows: Section 2 presents the framework in which our tracking methods are developed. In Section 3 we describe the tracking methods, with particular attention to the amplitude likelihoods. We also describe the detection process preceding target tracking, and how the various quantities involved are estimated. A conclusion is given in Section 4. Details regarding the numerical evaluation of the amplitude likelihoods are left for the Appendix. Simulation results are published in a separate paper [6].

2 Conceptual framework

In this paper we restrict attention to the single-target tracking problem. Although the real world most often poses problems that are suitably viewed as multiple target problems, the single-target problem must be properly understood before one can move onto multiple target problems. The utilization of AI is one such challenge where significant progress can and should be made in the single-target case.

The single-target tracking problem can be phrased in terms of the optimal Bayes equations,

$$\begin{aligned} p(\boldsymbol{x}_k|\boldsymbol{Z}^{k-1}) &= \int p(\boldsymbol{x}_k|\boldsymbol{x}_{k-1})p(\boldsymbol{x}_{k-1}|\boldsymbol{Z}^{k-1})\mathrm{d}\boldsymbol{x}_{k-1}, \\ p(\boldsymbol{x}_k|\boldsymbol{Z}^{k}) &\propto p(\boldsymbol{Z}_k|\boldsymbol{x}_k)p(\boldsymbol{x}_k|\boldsymbol{Z}^{k-1}). \end{aligned} \quad (1)$$

Our objective is to evaluate the posterior Probability Density Function (PDF) $p(\boldsymbol{x}_k|\boldsymbol{Z}^k)$ from the set of received measurements $\boldsymbol{Z}^k = \{\boldsymbol{Z}_1, \ldots, \boldsymbol{Z}_k\}$ where each $\boldsymbol{Z}_k$ contains m_k measurement vectors: $\boldsymbol{Z}_k = \{\boldsymbol{\zeta}_k(i)\}_{i=1}^{m_k}$. This is done using models for the likelihood $p(\boldsymbol{Z}_k|\boldsymbol{x}_k)$ and the transition prior $p(\boldsymbol{x}_k|\boldsymbol{x}_{k-1})$.

2.1 Kinematics

The kinematic state $\boldsymbol{x}_k$ will typically contain position and velocity, and possibly accelerations, heading, maneuver strengths etc. For easy of presentation we assume a linear kinematic transition prior,

$$\boldsymbol{x}_k = \boldsymbol{F}\boldsymbol{x}_{k-1} + \boldsymbol{v}_k, \;\; \boldsymbol{v}_k \sim \mathcal{N}(\boldsymbol{0}, \boldsymbol{Q}). \quad (2)$$

The tracking literature provides no established model for the development of the mean target power d_k through time. As the fluctuations of signal strength from scan to scan can be very severe, such fluctuations should be accounted for in the measurement model and not in the process model. It is very difficult to estimate a time-varying target power accurately for fluctuating targets [14]. It makes more sense to talk about the target power as something being constant over several (say ≥ 20) data frames. Therefore we treat the target power state as a constant parameter and write $d_k = d_{k-1} = d$.

2.2 Measurement model

We parameterize the measurement vector into a kinematic part $\boldsymbol{z}_k(i)$, an amplitude part $a_k(i)$ and a background part $\boldsymbol{q}_k(i)$ so that

$$\boldsymbol{\zeta}_k(i) = [\boldsymbol{z}_k^T(i), a_k(i), \boldsymbol{q}_k^T(i)]^T. \quad (3)$$

In order to make the estimation problem well-posed we assume that at most one measurement $\boldsymbol{\zeta}_k(i)$ can originate from the target. All the other measurements are thus considered as false alarms. We also assume that the mapping $\boldsymbol{x} \to \boldsymbol{z}$

is linear, for example through application of the coordinate transform described in [4],

$$\boldsymbol{z}_k = \boldsymbol{H}\boldsymbol{x}_k + \boldsymbol{w}_k, \;\; \boldsymbol{w}_k \sim \mathcal{N}(\boldsymbol{0}, \boldsymbol{R}). \tag{4}$$

The amplitudes $a_k(i)$ are under the hypotheses of noise or a target embedded in noise assumed to be distributed according to likelihoods $p_0(a_k(i) \,|\, \boldsymbol{q}_k(i))$ or $p_1(a_k(i) \,|\, d_k, \boldsymbol{q}_k(i))$ respectively. These will be thoroughly discussed in Sections 3.6 and 3.7.

2.3 The CLT and the Rayleigh model

The background model most often encountered in the tracking literature is the Rayleigh distribution, which is valid under the Central Limit Theorem (CLT). The backscattered signal z_k^i in resolution cell i has under the CLT a complex Gaussian distribution. The envelope or amplitude a is then Rayleigh distributed,

$$a = |z| \sim \mathrm{Ra}(a\,;\,\eta) \triangleq \frac{a}{\eta}\exp\left(\frac{-(a)^2}{2\eta}\right) \tag{5}$$

where η is the power of the background.

2.4 The K-distribution

The CLT is valid under the assumption of a large and non-random number of independent scatterers [13]. In reality the number of significant scatterers per resolution cell may not be high enough for the CLT to hold. One often observes a more heavy-tailed background than expected according to the CLT. The possibly most popular model for such non-Rayleigh clutter is the K-distribution [15]. A K-distributed amplitude a has the PDF

$$\mathrm{KPDF}\,(a\,;\,\nu, b) \triangleq \frac{4a^\nu}{\sqrt{b}^{\nu+1}\Gamma(\nu)} K_{\nu-1}\left(\frac{2a}{\sqrt{b}}\right). \tag{6}$$

For $\nu \to \infty$ the K-distribution turns into the Rayleigh distribution, while $\nu < 1$ indicates a very heavy-tailed background. By $\Gamma(\cdot)$ we denote the Gamma function while $K_\nu(\cdot)$ refers to the modified Bessel function of the second kind [10].

The K-distribution is popular for two reasons: Physical plausibility and mathematical convenience. The first reason has to do with the fact that reasoning similar to the CLT leads to the K-distribution [2,15].

In contrast to so-called stable distributions, the K-distribution has finite moments,

$$m_n = E\left[a^n\right] = \sqrt{b}^n \frac{\Gamma\left(1+\frac{n}{2}\right)\Gamma\left(\nu+\frac{n}{2}\right)}{\Gamma(\nu)}.$$

It is also convenient that the K-distribution can be viewed as a Rayleigh distribution $\mathrm{Ra}(a\,;\,\eta)$ modulated by a Gamma distribution $\mathrm{Ga}(\eta\,;\,\nu, b/2)$. In mathematical terms,

$$\begin{aligned} p(\eta\,;\,\nu, b) &= \mathrm{Ga}(\eta\,;\,\nu, b/2) \triangleq \frac{\eta^{\nu-1}\exp\left(-\frac{2\eta}{b}\right)}{(b/2)^\nu\,\Gamma(\nu)}, \\ p(a|\eta) &= \mathrm{Ra}(a\,;\,\eta), \\ \Rightarrow p(a\,;\,\nu, b) &= \mathrm{KPDF}\,(a\,;\,\nu, b)\,. \end{aligned} \tag{7}$$

This has motivated researchers to introduce the compound K-model [15], in which radar sea clutter is modeled by treating η as a correlated "texture" component, while $a|\eta$ is an uncorrelated "speckle" component. We let η refer to both the deterministic Rayleigh parameter in (5) and to the texture random variable in (7). The context will make it clear how η is supposed to be interpreted.

2.5 Model for target plus clutter

The compound interpretation of the K-distribution allows us to evaluate the PDF of a Swerling I target in K-distributed clutter as follows. Conditioned on the texture η, the background "noise" w has a complex zero-mean Gaussian PDF,

$$p(w|\eta) = \mathcal{N}_c(\eta) \triangleq \mathcal{N}\left(\begin{bmatrix} \mathrm{Re}(w) \\ \mathrm{Im}(w) \end{bmatrix}; \begin{bmatrix} 0 \\ 0 \end{bmatrix}, \begin{bmatrix} \eta & 0 \\ 0 & \eta \end{bmatrix}\right).$$

The complex backscatter signal s from a Swerling I target with power d also is Gaussian,

$$p(s|d) = \mathcal{N}_c(d).$$

Therefore the sum $z = s + w$ of signal and noise conditioned on η is Gaussian as well, and the corresponding amplitude $a = |z|$ is Rayleigh,

$$p(z|d,\eta) = \mathcal{N}_c(d+\eta) \Rightarrow p(a|d,\eta) = \mathrm{Ra}(d+\eta).$$

Under the compound K-model the texture η is random, so the PDF of the amplitude must be found by marginalizing over η,

$$\begin{aligned} p(a|d,\nu,b) &= \int_0^\infty \mathrm{Ga}\left(\eta;\nu,\frac{b}{2}\right)\mathrm{Ra}(a;d+\eta)\mathrm{d}\eta \\ &= \frac{a}{b^\nu\Gamma(\nu)}\int_0^\infty \frac{\eta^{\nu-1}}{\eta+d}\exp\left(-\frac{\eta}{b}-\frac{a^2}{2(\eta+d)}\right)\mathrm{d}\eta. \end{aligned} \tag{8}$$

3 Methodology

Most tracking systems employ a modularized architecture in which a detector extracts measurements to be fed to the data association and state estimation methods. This does not necessarily have to be the case, as exemplified by TBD methods which do not carry out any measurement extraction at all. Although our work is relevant for such methods as well [5], we are in this paper content with the modularized architecture as represented by the PDAF and the PDAFAI methods.

3.1 Extraction for Rayleigh case

For any cell i a detection is declared if its amplitude exceeds a certain threshold T_{Rk}^i. The detection threshold T_{Rk}^i is determined from a set of M auxiliary cells G_R^i according to the closed form formulas

$$\widehat{\eta}_k^i = \frac{1}{2M}\sum_{j\in G_R^i}(a_k^j)^2 \tag{9}$$

$$T_{Rk}^i = \sqrt{2M\left(\left(\frac{1}{P_{\mathrm{FA}}}\right)^{\frac{1}{M}} - 1\right)\cdot\widehat{\eta}_k^i}. \tag{10}$$

Here $\hat{\eta}_k^i$ is the Maximum Likelihood Estimator (MLE) of the background strength. The detector given by (9) and (10) gives an actual false alarm equal to the design false alarm rate P_{FA} as long as the background is Rayleigh. It is therefore referred to as a CFAR (Constant False Alarm Rate) detector [9].

The set of auxiliary cells is chosen to lie in the vicinity of the cell under test, although with guardbands to prevent them from being affected by signal leakage.

Each extracted measurement vector contains the location of the detected cell, as well as the value of the cell and the clutter estimate from its auxiliary cells. As discussed in Section 2.2, range and bearing can be converted to cartesian coordinates using simple formulas [4]. The full measurement vector of (3) is under the assumption of a Rayleigh background parameterized as

$$\boldsymbol{\zeta}(i) = [\boldsymbol{z}^T(i), a(i), \hat{\eta}(i)]^T.$$

Here $\boldsymbol{z}(i) = [\tilde{x}(i), \tilde{y}(i)]^T$ is the centroid of resolution cell number i in the cartesian coordinate system, which may or may not be related to the target through a model such as (4).

3.2 Extraction for K-case

If the background is significantly heavy-tailed, the detector given by (10) becomes increasingly inadequate. Instead of attempting to estimate the local background power η, we will estimate the K-distribution parameters ν and b from a somewhat larger set of N auxiliary cells, and then set the threshold according to the design false alarm rate for a K-distribution with these parameters. A Method of Moments (MoM) estimator recommended by [2] uses the first and the second moments of the data given by

$$m_1^i = \frac{1}{N}\sum_{j\in G_K^i} a_k^j \text{ and } m_2^i = \frac{1}{N}\sum_{j\in G_K^i} (a_k^j)^2.$$

This estimator attempts to solve the equation

$$\frac{m_2}{m_1^2} = \frac{4\nu\Gamma^2(\nu)}{\Gamma\left(\nu+\frac{1}{2}\right)}. \tag{11}$$

Since no closed form solution can be found the equation must be solved numerically. As explained in [2] a second-order approximation can be found as

$$\hat{\nu} = \frac{1}{4}\left[\log\left(\frac{\pi m_2}{4m_1^2}\right)\right]^{-1}. \tag{12}$$

While [2] recommends (12) as a starting point for the numerical search, we simply use (12) as our estimator of ν. Figure 2 shows that for very heavy-tailed clutter ($\nu \approx 0.1$) the estimator (12) has a significant bias, and the numerical search is necessary in order to obtain an unbiased estimator. But for moderately heavy-tailed clutter ($\nu \geq 0.5$) the numerical search appears to be overkill. Having estimated ν, we estimate b as

$$\hat{b} = m_2/\hat{\nu}. \tag{13}$$

We can now for any resolution cell i determine a threshold T_K^i according to the criterium

$$P(a > T_K) \approx 1 - \frac{2a^\nu}{\sqrt{b}^\nu\Gamma(\nu)}K_\nu\left(\frac{2T_K}{\sqrt{b}}\right) = P_{\text{FA}}. \tag{14}$$

This is a nonlinear equation in T_K which must be solved numerically. Instead of working directly with the cumulative distribution function as in (14), we recommend using the square of its logarithm for numerical stability.

A test using the threshold T_K is carried out in order to decide whether cell i should be stored among the detected measurements. When a K-distributed background is assumed we must store two background estimates for each measurement vector. In addition it is convenient to store the detection threshold $T_K(i)$:

$$\begin{aligned}\boldsymbol{\zeta}(i) =& [\boldsymbol{z}^T(i), a(i), \hat{\nu}(i), \hat{b}(i), T_K(i)]^T \\ \triangleq& [\boldsymbol{z}^T(i), a(i), \boldsymbol{q}(i)]^T.\end{aligned}$$

3.3 Probabilistic Data Association

The PDAF [4] is perhaps today's most popular tracking algorithm due to its pragmatic compromise between efficiency and robustness. It is a suboptimal algorithm which at each time step collapses the target state posterior PDF into a single Gaussian which then is propagated to the next time step. Thus the past information about the target at time step k can be summarized by

$$p(\boldsymbol{x}_k|\boldsymbol{Z}^{k-1}) \approx \mathcal{N}(\boldsymbol{x}_k\,;\,\hat{\boldsymbol{x}}_{k|k-1}, \boldsymbol{P}_{k|k-1}). \tag{15}$$

The lumping (cf. Figure 1) implied by (15) is done by expressing the state estimate at time k as a weighted average of the prediction $\hat{\boldsymbol{x}}_{k|k-1}$ and state estimates conditioned on the latest measurements $\boldsymbol{z}_k(i)$. This leads to the following Kalman Filter-like equations for prediction and measurement update of the state estimate $\hat{\boldsymbol{x}}_{k|k}$ and its associated covariance $\boldsymbol{P}_{k|k}$:

$$\begin{aligned}\hat{\boldsymbol{x}}_{k|k-1} &= \boldsymbol{F}\hat{\boldsymbol{x}}_{k-1|k-1}, \\ \boldsymbol{P}_{k|k-1} &= \boldsymbol{F}\boldsymbol{P}_{k-1|k-1}\boldsymbol{F}^T + \boldsymbol{Q} \\ \hat{\boldsymbol{x}}_{k|k} &= \hat{\boldsymbol{x}}_{k|k-1} + \boldsymbol{K}_k\sum_{i=1}^{m_k}\beta_k(i)\boldsymbol{\nu}_k(i) \\ \boldsymbol{P}_{k|k} &= \boldsymbol{P}_{k|k-1} - (1-\beta_k(0))\boldsymbol{K}_k\boldsymbol{S}_{k|k-1}\boldsymbol{K}_k^T + \tilde{\boldsymbol{P}}_k\end{aligned} \tag{16}$$

where

$$\begin{aligned}\boldsymbol{K}_k &= \boldsymbol{P}_{k|k-1}\boldsymbol{H}^T\boldsymbol{S}_{k|k-1}^{-1} \\ \boldsymbol{S}_{k|k-1} &= \boldsymbol{H}\boldsymbol{P}_{k|k-1}\boldsymbol{H}^T + \boldsymbol{R}_k \\ \boldsymbol{\nu}_k(i) &= \boldsymbol{z}_k(i) - \boldsymbol{H}\hat{\boldsymbol{x}}_{k|k-1} = \boldsymbol{z}_k(i) - \hat{\boldsymbol{z}}_{k|k-1} \\ \tilde{\boldsymbol{P}}_k &= \boldsymbol{K}_k\left[\sum_{i=1}^{m_k}\beta_k(i)\boldsymbol{\nu}_k(i)\boldsymbol{\nu}_k(i)^T - \boldsymbol{\nu}_k\boldsymbol{\nu}_k^T\right]\boldsymbol{K}_k^T \\ \boldsymbol{\nu}_k &= \sum_{i=1}^{m_k}\beta_k(i)\boldsymbol{\nu}_k(i).\end{aligned}$$

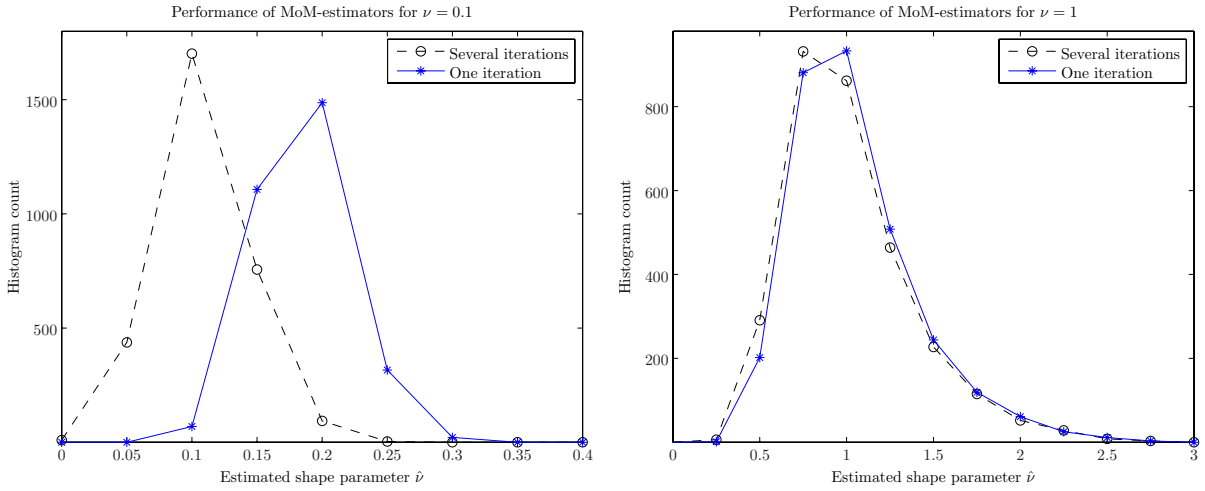

Figure 2: Histograms illustrating the distributions of $\hat{\nu}$ when the true shape parameter is 0.1 or 1.

The index i ranges over all m_k extracted and validated measurements inside a validation gate around $\hat{\boldsymbol{z}}_{k|k-1}$. The validation gate is defined by the criterium

$$\left(\boldsymbol{z}_k(i) - \hat{\boldsymbol{z}}_{k|k-1}\right)^T \boldsymbol{S}_k^{-1} \left(\boldsymbol{z}_k(i) - \hat{\boldsymbol{z}}_{k|k-1}\right) < g^2,$$

where the gate threshold g typically has a value in the interval between 3 and 10.

Derivations of the association weights $\beta_k(i)$ can be found in [4]. In the conventional case without AI they are written

$$\beta_k(i) = \begin{cases} \frac{e(i)}{b + \sum_{j=1}^{m_k} e(j)} & i = 1, \ldots, m_k \\ \frac{b}{b + \sum_{j=1}^{m_k} e(j)} & i = 0 \end{cases}, \qquad (17)$$

where

$$e(i) = e^{-\left(\boldsymbol{z}_k(i) - \hat{\boldsymbol{z}}_{k|k-1}\right)^T \boldsymbol{S}_k^{-1} \left(\boldsymbol{z}_k(i) - \hat{\boldsymbol{z}}_{k|k-1}\right)/2}.$$

The value of b depends on the model for the false alarm point process. The parametric version of the PDAF assumes that the number of false alarms has a Poisson distribution with parameter λV, where V is the volume of the validation gate and λ is the spatial clutter density. It can then be shown that [4]

$$b = (2\pi/g)^{\frac{n_{\boldsymbol{z}}}{2}} \lambda V (1 - P_{\mathrm{D}} P_{\mathrm{G}})/(c_{n_{\boldsymbol{z}}} P_{\mathrm{D}}).$$

For the more robust non-parametric version of the PDAF we replace λV by m_k, thereby yielding

$$b = (2\pi/g)^{\frac{n_{\boldsymbol{z}}}{2}} m_k (1 - P_{\mathrm{D}} P_{\mathrm{G}})/(c_{n_{\boldsymbol{z}}} P_{\mathrm{D}}).$$

3.4 PDAF with Amplitude Information

In [11] it was suggested to improve the performance of the PDAF algorithm by using the amplitude of the measurements as part of the tracking algorithm. The amplitude information only affects the association weights and not the state estimation itself, as illustrated in Figure 1. The modified association weights are given by

$$\begin{aligned} e(i) &= e^{-\left(\boldsymbol{z}_k(i) - \hat{\boldsymbol{z}}_{k|k-1}\right)^T \boldsymbol{S}_k^{-1} \left(\boldsymbol{z}_k(i) - \hat{\boldsymbol{z}}_{k|k-1}\right)/2} \\ &\quad \cdot \left[p_1(a_k(i)|\hat{d}_k, \hat{\boldsymbol{q}}_k(i)) \,/\, P_{\mathrm{D}}\right] / \left[p_0(a_k(i)|\hat{\boldsymbol{q}}_k(i)) \,/\, P_{\mathrm{FA}}\right] \\ &\triangleq e^{-\left(\boldsymbol{z}_k(i) - \hat{\boldsymbol{z}}_{k|k-1}\right)^T \boldsymbol{S}_k^{-1} \left(\boldsymbol{z}_k(i) - \hat{\boldsymbol{z}}_{k|k-1}\right)/2} \\ &\quad \cdot l(a_k(i)|\hat{d}_k, \hat{\boldsymbol{q}}_k(i)), \end{aligned}$$

where the amplitude likelihood ratio $l(a_k(i)|\hat{d}_k, \hat{\boldsymbol{q}}_k(i))$ depends on the observed amplitude $a_k(i)$, the target power estimate $\hat{d}_k$ and a description of the background which is contained in $\hat{\boldsymbol{q}}_k(i)$.

The likelihoods $p_0(\ldots)$ and $p_1(\ldots)$ are the PDF's of the amplitude under the two hypotheses of only clutter and of clutter plus a target with power $\hat{d}_k$. Their exact expressions depend on how the background is modeled. Notice that $p_0(\ldots)$ and $p_1(\ldots)$ are divided by P_{FA} and P_{D} respectively in order to compensate for the fact that $a_k(i)$ has exceeded the detection threshold.

3.5 The target power

Under the Rayleigh assumption an MoM estimator $\hat{d}_k$ of the mean target power d at time step k can be written

$$\widehat{d_k} = \max\left(\frac{C_k}{D_k}, \frac{B_k - C_k}{D_k}\right) \qquad (18)$$

where

$$\begin{aligned} B_k &= \frac{1}{2L}\left(\sum_{l=1}^{L} \frac{1}{m_{k-l+1}} \sum_{i=1}^{m_{k-l+1}} a_{k-l+1}^2(i)\beta_{k-l+1}(i)\right) \\ C_k &= \frac{1}{L}\left(\sum_{l=1}^{L} \frac{1}{m_{k-l+1}} \sum_{i=1}^{m_{k-l+1}} \hat{\eta}_{k-l+1}(i)\beta_{k-l+1}(i)\right) \\ D_k &= \frac{1}{L}\sum_{l=1}^{L}(1 - \beta_{k-l+1}(0)). \end{aligned}$$

This estimator, which is developed in [7], is also used to estimate the target power when the background is K-distributed. Then $\hat{\eta}_{k-l+1}(i)$ is found as half the second moment, or equivalently

$$\hat{\eta}_{k-l+1}(i) = \frac{\hat{\nu}_{k-l+1}(i)\hat{b}_{k-l+1}(i)}{2}. \tag{19}$$

The time lag L is a tuning constant whose optimal value hardly can be determined rigorously. It would need to be rather large in order to provide an accurate estimate of d. On the other hand, permanent changes in the target amplitude may in practice occur quite abruptly. As a compromise we have found $L = 20$ to be a reasonable value. When the track is younger than L time steps (i.e. $k < L$) we necessarily use a shorter lag.

The amplitude estimate plays a fundamental role in the likelihood ratio introduced in Section 3.4. It is also useful in order to determine the expected probability of detection P_{D}. For the case of a Swerling I target in Rayleigh clutter we find the detection probability as

$$P_{\mathrm{D}} = \left(1 + \left(P_{\mathrm{FA}}^{-1/M} - 1\right)\frac{\eta}{d+\eta}\right)^{-M}.$$

When the clutter is K-distributed we find the detection probability by reasoning analogous to (8) as

$$P_{\mathrm{D}} = \frac{(2/b)^{\nu}}{\Gamma(\nu)}\int_0^{\infty} \eta^{\nu-1}\exp\left(-\frac{2}{b}\eta - \frac{T_K^2}{2(\eta+d)}\right)\mathrm{d}\eta \tag{20}$$

where T_K is the detection threshold as obtained from (14). How to evaluate (20) efficiently is explained in the Appendix.

3.6 Likelihoods for Rayleigh case

Under the Rayleigh-Swerling I assumption used in [11] the likelihoods of Section 3.4 become

$$\begin{aligned} p_0(a|\eta) &= \frac{a}{\eta}\exp\left(\frac{-a^2}{2\eta}\right) \\ p_1(a|d,\eta) &= \frac{a}{(\eta+d)}\exp\left(\frac{-a^2}{2(\eta+d)}\right) \\ \Rightarrow l(a|d,\eta) &= \frac{P_{\mathrm{FA}}}{P_{\mathrm{D}}}\cdot\frac{\eta}{\eta+d}\cdot\exp\left(\frac{a^2 d}{2\eta(\eta+d)}\right). \end{aligned} \tag{21}$$

The formula (21) is optimal given that the true values of d and η are known. Clearly (21) is not optimal if the Rayleigh assumption is inadequate, but it may still be used as a heuristic. Several papers starting with [11] have demonstrated the gain from (21) under ideal circumstances. The performance of (21) under less ideal circumstances has on the other hand not received much attention in the tracking literature.

In this section we suggest one possible strategy of coping with the inevitable uncertainty of η without introducing the K-distribution. This strategy is to account for the uncertainty of η in a way analogous to what is done in the CFAR threshold (10). In the context of TBD this has been shown to have a crucial impact on performance [5].

The estimator $\hat{\eta}$ given by (9) is a random variable with a corresponding PDF that should be accounted for in the likelihood evaluation. Its PDF $p(\hat{\eta}|\eta)$ depends on the true noise parameter η. To utilize the information carried in this PDF requires us to treat η as random as well and assign it a prior distribution $p(\eta)$. By marginalizing the joint distribution of a and η given $\hat{\eta}$ we obtain

$$p(a|d,\hat{\eta}) \propto \int p(a|d,\eta)p(\hat{\eta}|\eta)p(\eta)\mathrm{d}\eta. \tag{22}$$

The background estimate $\hat{\eta}$ given by (9) is under the assumption of independent Rayleigh samples known to follow a Gamma distribution,

$$p(\hat{\eta}|\eta) = \mathrm{Ga}\left(M, \frac{\eta}{M}\right) = \frac{\hat{\eta}^{M-1}\exp\left(-\frac{\hat{\eta}M}{\eta}\right)}{\left(\frac{\eta}{M}\right)^M\Gamma(M)}.$$

Since we do not have any more prior information than the value of $\hat{\eta}$ itself we use a flat and thus non-informative prior in the Rayleigh case:

$$p(\eta) = \mathrm{Uniform}(\eta;[0,\xi]). \tag{23}$$

Here ξ is a very large number. The flat prior allows us to use $p(\hat{\eta}|\eta)$ without being bothered by $p(\eta)$. The likelihood ratio becomes

$$\begin{aligned} l(a|d,\hat{\eta}) &= \frac{P_{\mathrm{FA}}}{P_{\mathrm{D}}}\cdot\frac{p(a|d,\hat{\eta})}{p(a|0,\hat{\eta})} \\ &= \frac{P_{\mathrm{FA}}}{P_{\mathrm{D}}}\frac{\int_0^{\xi}\mathrm{Ra}\left(a\,;\,\eta+d\right)\mathrm{Ga}\left(\hat{\eta}\,;\,M,\frac{\eta}{M}\right)\mathrm{d}\eta}{\int_0^{\xi}\mathrm{Ra}\left(a\,;\,\eta\right)\mathrm{Ga}\left(\hat{\eta}\,;\,M,\frac{\eta}{M}\right)\mathrm{d}\eta}. \end{aligned} \tag{24}$$

For $\xi \to \infty$ we obtain

$$\begin{aligned} l(a|d,\hat{\eta}) = \frac{P_{\mathrm{FA}}}{P_{\mathrm{D}}}\cdot\frac{\Gamma(M)}{\left[\hat{\eta}M + \frac{a^2}{2}\right]^M} \\ \cdot\int_0^{\infty}\frac{1}{(\eta)^M(\eta+d)}\exp\left(-\frac{\hat{\eta}M}{\eta} - \frac{a^2}{2(\eta+d)}\right)\mathrm{d}\eta. \end{aligned} \tag{25}$$

The Appendix explains how this expression can be evaluated in an efficient way.

3.7 Likelihood for K-case

Significant heavy-tailedness is under the compound K-model (7) treated by assigning a Gamma prior distribution to η. The uncertainty imposed on η this way is likely to be more severe than the uncertainty induced by the CFAR background estimate (9). Therefore it is not of primary importance to account for estimation uncertainty in the proper treatment of K-distributed clutter. Rather we simply evaluate $p_1(a|d,\nu,b)$ and $p_0(a|\nu,b)$ under the compound K-

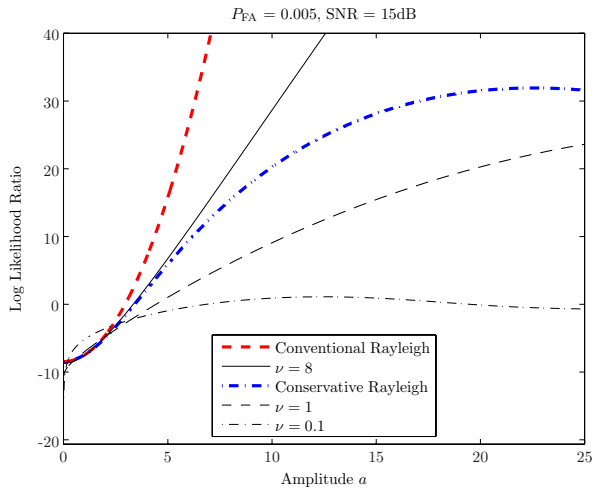

Figure 3: Various likelihoods for SNR = 15dB.

model (7) as done in (8). This yields

$$\begin{aligned} p_0(a) =& \frac{4a^\nu}{\sqrt{b}^{\nu+1}\Gamma(\nu)} K_{\nu-1}\left(\frac{2a}{\sqrt{b}}\right), \\ p_1(a) =& \frac{a}{b^\nu\Gamma(\nu)} \int_0^\infty \frac{\eta^{\nu-1}}{\eta+d} \exp\left(-\frac{\eta}{b} - \frac{a^2}{2(\eta+d)}\right) \mathrm{d}\eta, \\ \Rightarrow l(a) =& \frac{P_{\mathrm{FA}}}{P_{\mathrm{D}}} \cdot \frac{(a\sqrt{b})^{1-\nu}}{4K_{\nu-1}\left(\frac{2a}{\sqrt{b}}\right)} \\ & \cdot \int_0^\infty \frac{\eta^{\nu-1}}{\eta+d} \exp\left(-\frac{\eta}{b} - \frac{a^2}{2(\eta+d)}\right) \mathrm{d}\eta. \end{aligned} \quad (26)$$

The integral in (26) must be solved numerically, as outlined in the Appendix.

Figure 3 shows the log likelihood ratios $\ln l(a|\ldots)$ corresponding to (21), (25) and (26) for various shape parameters ν. Assuming that our estimate of the target power d corresponds to a target with SNR = 15dB, the curves show the log likelihood ratios as functions of the actual amplitude value. Heavy-tailed noise is seen to lead to a more conservative likelihood. For really spiky clutter ($\nu \approx 0.1$) the log likelihood ratio curve corresponding to (26) hardly exceeds zero. This tells us that tracking a 15dB target in such noise most likely is futile. For $\nu = 8$ the behavior of (26) is not very different from (21), which means that the Rayleigh approximation may be considered adequate. The behavior of (25) is on the other hand always qualitatively different from (21). It saturates and even falls back for very large a.

4 Conclusion

In this paper the classical PDAF method has been tailored to cope with heavy-tailed clutter. In particular we have developed conservative likelihoods which evaluate amplitude information in a robust way. The actual performance of these developments is investigated in [6].

Appendix: Likelihood evaluations

The tracking methods developed in this paper rely on evaluations of the integrals in (20), (25) and (26). Although no closed-form solutions exist to any of these integrals, they can be evaluated quite fast within a reasonable accuracy. How this can be done is explained in this appendix.

According to [12], the integral in (26) is "readily integrated numerically". However, the integrand has several undesirable properties which must be addressed. On the one hand it may tend quickly towards ∞ as $\eta \to 0$, while on the other hand it may tend very slowly towards 0 as $\eta \to \infty$. Its overall shape is difficult to characterize in simple formulas. The popular strategy of importance sampling is likely to fail since the obvious factorization may lead to factors with effectively disjunct supports.

To overcome these challenges we use the substitution

$$\eta = \frac{1}{u^2} \quad \Rightarrow \quad \mathrm{d}\eta = -\frac{2}{u^3}\mathrm{d}u, \quad (27)$$

and express the likelihood ratio as

$$\begin{aligned} l(a|d,\nu,b) =& \frac{P_{\mathrm{FA}}}{P_{\mathrm{D}}} \cdot \frac{(a\sqrt{b})^{1-\nu}}{2K_{\nu-1}\left(\frac{2a}{\sqrt{b}}\right)} \\ & \cdot \int_0^\infty \frac{u^{1-2\nu}}{1+u^2 d} \exp\left(-\frac{2}{u^2 b} - \frac{u^2 a^2}{1+u^2 d}\right) \mathrm{d}u. \end{aligned} \quad (28)$$

Denoting the two integrands $g(\eta)$ and $g^*(u)$, we see in Figure 4 that the behavior of $g^*(u)$ is more regular than the behavior of $g(\eta)$. The modified integrand $g^*(u)$ is integrated numerically over two grids. A lower grid with fixed resolution captures the behavior of $g^*(u)$ around its peak, which is given by a cubic equation. An upper grid with exponentially decreasing resolution captures its asymptotic behavior. Exact formulas for the grids are given in [7], but will be left out here for the sake of brevity.

Using the substitution (27) in (20) we express the K-Swerling I detection probability as

$$P_{\mathrm{D}} = \frac{2(2/b)^\nu}{\Gamma(\nu)} \int_0^\infty \frac{1}{u^{2\nu+1}} \exp\left(-\frac{2}{u^2 b} - \frac{u^2 T_K^2}{2(1+u^2 d)}\right) \mathrm{d}u.$$

This modified integrand has a behavior similar to $g^*(u)$, and the same technique with two sampling grids can be used.

The substitution (27) also makes the integral in (25) more well-behaved:

$$\begin{aligned} l(a|d,\hat{\eta}) =& \frac{P_{\mathrm{FA}}}{P_{\mathrm{D}}} \cdot \frac{\Gamma(M)}{\left[\hat{\eta}M + \frac{a^2}{2}\right]^M} \\ & \cdot \int_0^\infty \frac{u^{2M-1}}{1+u^2 d} \exp\left(-u^2\left[\hat{\eta}M + \frac{a^2}{2(1+u^2 d)}\right]\right) \mathrm{d}u. \end{aligned}$$

For this integral the grid is constructed by placing 100 sample points uniformly on the interval $u \in [0, \sqrt{1/\hat{\eta}}]$.

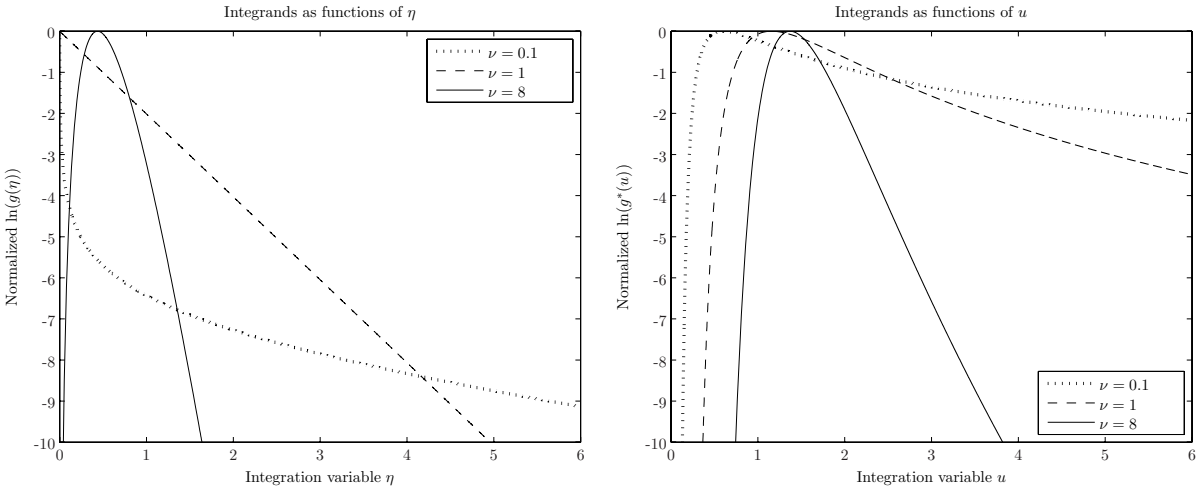

Figure 4: Example integrands of the K-Swerling I likelihood plotted as functions of the texture variable η and $u = 1/\sqrt{\eta}$. The amplitude is $a = 5$ and the expected SNR is $15\mathrm{dB}$ for all three cases. The scale parameter b is $1/\nu$ in order to keep the second moment of the background equal to one.

References

[1] D. Abraham, "Choosing a Non-Rayleigh Reverberation Model," in *OCEANS '99 MTS/IEEE. Riding the Crest into the 21st Century*, vol. 1, Seattle, WA, Sep. 1999, pp. 284–288.

[2] D. Abraham and A. Lyons, "Novel Physical Interpretations of K-Distributed Reverberation," *IEEE Journal of Oceanic Engineering*, vol. 27, no. 4, pp. 800–813, Oct. 2002.

[3] B. Armstrong and H. Griffiths, "CFAR detection of fluctuating targets in spatially correlated K-distributed clutter," *IEE Proceedings F Radar and Signal Processing*, vol. 138, no. 2, pp. 139–152, Apr. 1991.

[4] Y. Bar-Shalom and X. R. Li, *Multitarget-Multisensor Tracking: Principles and Techniques*. Storrs, CT, USA: YBS Publishing, 1995.

[5] E. Brekke, T. Kirubarajan, and R. Tharmarasa, "Tracking Dim Targets Using Integrated Clutter Estimation," in *Proceedings of SPIE*, vol. 6699, San Diego, CA, United States, Aug. 2007.

[6] E. Brekke, O. Hallingstad, and J. Glattetre, "Performance of PDAF-based Tracking Methods in Heavy-Tailed Clutter," to appear in Proceedings of the 12th International Conference on Information Fusion.

[7] ——, "Tracking Small Targets in Heavy-Tailed Clutter Using Amplitude Information," submitted to IEEE Journal of Oceanic Engineering.

[8] T. Bucciarelli, P. Lombardo, and S. Tamburrini, "Optimum CFAR detection against compound Gaussian clutter with partially correlated texture," *IEE Proceedings: Radar, Sonar and Navigation*, vol. 143, no. 2, pp. 95–104, Apr. 1996.

[9] P. P. Gandhi and S. A. Kassam, "Analysis of CFAR Processors in Non-Homogeneous Background," *IEEE Transactions on Aerospace and Electronic Systems*, vol. 24, no. 4, pp. 427–445, Jul. 1988.

[10] I. Gradshteyn and I. Ryzhik, *Table of Integrals, Series, and Products*, 7th ed., D. Zwillinger, Ed. Academic Press, Elsevier Inc., 2007.

[11] D. Lerro and Y. Bar-Shalom, "Interacting Multiple Model Tracking with Target Amplitude Feature," *IEEE Transactions on Aerospace and Electronic Systems*, vol. 29, no. 2, pp. 494–509, Apr. 1993.

[12] D. Middleton, "New Physical-Statistical Methods and Models for Clutter and Reverberation: the KA-Distribution and Related Probability Structures," *IEEE Journal of Oceanic Engineering*, vol. 24, no. 3, pp. 261–284, Jul. 1999.

[13] A. Papoulis and S. U. Pillai, *Probability, Random Variables and Stochastic Processes*. McGraw-Hill, 2002.

[14] M. G. Rutten, N. J. Gordon, and S. Maskell, "Recursive track-before-detect with target amplitude fluctuations," in *IEE Proceedings: Radar, Sonar and Navigation*, vol. 152, Oct. 2005, pp. 345–352.

[15] K. D. Ward, R. J. A. Tough, and S. Watts, *Sea Clutter: Scattering, the K Distribution and Radar Performance*, ser. IET Radar, Sonar and Navigation Series. London, UK: The Institution of Engineering and Technology, 2006, vol. 20.